



ACCEPTED ON ANNALS OF GEOPHYSICS, 61, 2018; Doi:
10.4401/ag-7925

The contribution of the Istituto Nazionale di Geofisica e Vulcanologia (INGV) to “Adria LithosPHere investigAtion (ALPHA)” active seismic experiment

Luigi Improta^{*1}, Milena Moretti¹, Aladino Govoni¹, Marina Pastori¹, Claudio Chiarabba¹, Pasquale De Gori¹, A. Dannowski², Heidrun Kopp^{2,3}

¹INGV (Istituto Nazionale di Geofisica e Vulcanologia, Osservatorio Nazionale Terremoti)

²GEOMAR (Helmholtz-Zentrum für Ozeanforschung Kiel)

³University of Kiel (Christian-Albrechts-Universität zu Kiel)

1 **The contribution of the Istituto Nazionale di Geofisica e Vulcanologia (INGV) to**
2 **“Adria LithosPHere investigAtion (ALPHA)” active seismic experiment**

3
4 Luigi Improta*¹, Milena Moretti¹, Aladino Govoni¹, Marina Pastori¹, Claudio Chiarabba¹, Pasquale
5 De Gori¹, A. Dannowski², Heidrun Kopp^{2,3}

6
7 *Corresponding author: Luigi Improta@ingv.it

8 ¹**INGV** (*Istituto Nazionale di Geofisica e Vulcanologia, Osservatorio Nazionale Terremoti*)

9 ²**GEOMAR** (*Helmholtz-Zentrum für Ozeanforschung Kiel*)

10 ³**University of Kiel** (*Christian-Albrechts-Universität zu Kiel*)

11

12	Index
13	Abstract
14	
15	1. The ALPHA Project and the 2012 active seismic survey
16	2. The INGV temporary seismic network: instrumentation and deployment
17	2.1 The profile onshore P02
18	2.2 The profile onshore P03
19	2.3 The instrumentation
20	3. Data description
21	3.1 Profile P02
22	3.2 Profile P03
23	4. Discussions and Conclusions
24	
25	
26	References
27	

28 **Abstract**

29

30 During the winter 2012, from 20 January to 4 February, the German oceanographic FS METEOR
31 cruise (M86/3) took place in the central-southern Adriatic Sea in the frame of “Adria LithosPHere
32 InvestigAtion” (ALPHA [Kopp et al., 2013]). The primary goal of the project was high-resolution
33 tomographic imaging of the crust and lithospheric mantle underneath the southern Adriatic Sea, the Apulia
34 eastern margin and the external zone of the Dinaric thrust-belt by collecting offshore-onshore seismic data
35 along three multi-fold wide-aperture profiles. The definition of reliable velocity models of the Adriatic
36 lithosphere was considered crucial for a better understanding of the structure, fragmentation, geodynamic
37 evolution, and seismotectonics of the Adria-Apulia microplates.

38 The ALPHA Project was coordinated by Helmholtz Centre for Ocean Research Kiel, Germany
39 (GEOMAR), former Leibniz Institute of Marine Sciences (German: Leibniz-Institut für
40 Meereswissenschaften, IFM-GEOMAR) and conducted in close cooperation with different European
41 institutions of Germany, Albania, Croatia, Italy and Montenegro. The Istituto Nazionale di Geofisica
42 Vulcanologia (INGV) participated by deploying land stations along two transects in the Apulia and Gargano
43 Promontory to extend westwards the seismic profiles. The primary goal was to record shallow-to-deep
44 seismic phases travelling along the transition between the Adriatic basin and the Apulia foreland.

45 In this paper we present the field work related to the two Italian onshore transects, the recorded data,
46 and the processing flow developed to highlight crustal and mantle refractions and wide-angle reflections.

47

48

49 **1. The ALPHA Project and the 2012 active seismic survey**

50

51 The “Adria LithosPHere InvestigAtion” (ALPHA [Kopp et al., 2013]) active seismic experiment was
52 performed during the winter 2012 (20 January – 04 February) in the central-southern Adriatic Sea and
53 surrounding onshore regions. The ALPHA Project was coordinated by GEOMAR (Kiel, Germany) and
54 conducted in close cooperation with German and European institutions (GFZ, ETH, Seismological
55 Observatory of Montenegro, University of Tirana, Istituto Nazionale di Geofisica e Vulcanologia - INGV,
56 Istituto di Scienze Marine of the Centro Nazionale delle Ricerche – ISMAR). The primary goal of the
57 experiment was high-resolution tomographic imaging of the southern Adriatic crust and lithosphere by using
58 active source marine data. Indeed, the lithospheric structure of Adria still remains mainly unresolved because
59 geophysical and seismic data were mainly acquired along the Periadriatic regions. Consequently, various
60 models of tectonic fragmentation and recent kinematic evolution have been proposed [Bennett et al., 2008].

61 The project aimed at filling this information gap by collecting mainly three multi-fold wide-aperture
62 seismic refraction profiles in the framework of FS METEOR cruise M86/3 in the central-southern Adriatic
63 Sea (Figure 1). The first profile (P01) entirely ran NW-SE in the middle of the central-southern Adriatic Sea
64 intercepting the Gargano-Dubrovnik shear zone that presumably separates the Adria microplate to the north
65 from the Apulia microplate to the south [D’Agostino et al., 2008]. The remaining two profiles extended SW-
66 NE from the coastline of the Apulia (P02) and W-E from the Gargano Promontory (P03) to the Dinaric
67 external front across the southern Adriatic sea (e.g. across the Apulia microplate). A total number of 36
68 Ocean Bottom Hydrophones (OBH) and Seismometers (OBS) were deployed along each profile with an
69 average spacing of ~5 km (P02) and ~6.5 km (P01 and P03). The OBH/OBS recorded the signals produced
70 by an array of 6 airguns for a total volume of 84 litres. The approximate shooting interval was 110 m (P02)
71 and 140 m (P01 and P03). The resulting offshore profiles measured a length of 245 km (P01), 180 km (P02)
72 and 220 km (P03). During the acquisition of profiles P02 and P03, land stations were installed both in Italy
73 and in Montenegro/Albania to record the offshore airgun shots. On-land deployments aimed at extending
74 further the maximum offset of observation that is a key parameter to record deep phases from the crust-
75 mantle boundary (Pn refractions and PmP post-critical reflections) and to obtain information on the crustal
76 structure in the Periadriatic zones.

77 Profiles P02 and P03 were extended westward by INGV's field team that deployed short-period
78 seismic stations across the Apulia and Gargano Promontory, respectively (Figure 1). The goal was to record
79 shallow-to-deep phases travelling across the transition between the Adriatic basin and the Apulia foreland.

80 In this manuscript we illustrate: (i) the onshore experiment, (ii) the processing flow developed to
81 improve data quality and highlight crustal and mantle refractions and wide-angle reflections, (iii) describe
82 the characteristics of first arrivals and main wide-angle reflected phases identified on the elaborated record
83 sections. In particular, we show that a careful frequency-time analysis of the data allowed to design optimal
84 filters aimed at identifying very weak first arrivals in the intermediate-large offset range. These steps of the
85 developed processing flow were of key importance because the recognition of primary head waves on the
86 record sections was hampered by shadow zones associated to low-Vp layers placed at the base of the Apulian
87 sedimentary cover.

88 89 90 **2. The INGV temporary seismic network: instrumentation and deployment**

91
92 We installed a total of thirteen temporary seismic stations along P02 and P03 profiles in Apulia and in
93 the Gargano Promontory. The deployment has been done in two stages and in close coordination with the
94 offshore activities:

95 a) the first transect of eight seismic stations was installed in Apulia along the onshore continuation of
96 the offshore profile P02 that strikes NE-SW. The transect extends from the Adriatic coastline (to the north of
97 Brindisi) to the Taranto gulf (to the south of Taranto; see Figure 2);

98 b) the second deployment consisted of five stations installed in the Gargano Promontory along the
99 onshore continuation of the offshore profile P03 that trends E-W (see Figure 3).

100 Potential recording sites were preliminarily identified inside a narrow strip surrounding the onshore
101 continuation of each profile by the analysis of aerial photos and geologic maps. Then, the definitive sites
102 were chosen after field inspections in the area of interest. All stations were deployed on limestone outcrops
103 and far from sources of cultural noise. To respect these conditions, the station spacing is not regular but this
104 allowed recording of very good quality data as described in the next paragraphs.

105 106 **2.1 The onshore segment of profile P02**

107 The onshore segment of profile P02 is approximately 55 km long and has an average station spacing
108 of about 6 km. Stations are 0.1 to 2.7 km distant from the onshore continuation of the profile (yellow line in
109 Figure 2). The first station (R1) was installed 2.7 km to the west of the Adriatic coastline, the last one (R8) at
110 a distance of 5 km to the east of the Ionian coastline. Distances from the closest airgun shot were: 7.8 km
111 (P02_R1), 15.5 km (P02_R2), 22.0 km (P02_R3), 27.2 km (P02_R4), 35.1 km (P02_R5), 40.8 km (P02_R6),
112 47.1 km (P02_R7) and 55.6 (P02_R8). Station elevations range from 20 m to 210 m.

113 All stations started recording prior to the expected shooting that would have begun on 20 January from
114 the Montenegro side of the profile. Due to the adverse weather conditions in the Adriatic Sea, the shooting
115 was delayed until 10:00 a.m. of 22 January and ended at 11:46 a.m. of 23 January. The average shot spacing
116 was 114 m. The sea floor depth along profile P02 is reported in Figure 4.

117 118 **2.2 The onshore segment of profile P03**

119 The onshore segment of profile P03 is about 33 km long. Station spacing was very irregular (the
120 station interval ranges from 2 to 7 km) due to the logistic difficulties and environmental conditions of the
121 Gargano mountainous area (yellow line in Figure 3). The first station (R1) was located 2.3 km to the west of
122 the coastline, the farther one (R5) at a distance of 23.7 km. Distances from the closest airgun shot were: 11.7
123 km (P03_R1), 17.1 km (P03_R2), 24.6 km (P03_R3), 26.6 km (P03_R4), 33.1 km (P03_R5). Station
124 elevations range from 104 m to 754 m. All stations started recording prior to the shooting that started from

125 the Gargano coastline at 07:28 a.m. of 27 January and ended at 11:22 a.m. of 28 January. The average source
126 spacing was 140 m. The sea floor depth along profile P03 is reported in Figure 4.

127

128

129 **2.3 The instrumentation**

130 We used a Reftek-130 24 bit digitizer (www.reftek.com) equipped with three components Lennartz
131 LE-3Dlite seismometer with a dominant period of 1s (<http://www.lennartz-electronic.de>) and a GPS antenna.
132 Each station was equipped with a battery of 40 Ah, sufficient for ten days of acquisition and removable disks
133 for local data storage.

134 The coordinates of the two final profile configurations are listed in Table 1 (profile P02) and Table 2
135 (profile P03). The sampling rate was fixed at 8 ms. Each seismometer was buried in a hole and deployed on a
136 concrete base.

137

138

139 **3. Data analysis and description**

140

141 **3.1 Data processing**

142 In order to define a processing flow aimed at enhancing the main crustal phases, post-critical wide-
143 angle reflections (PmP) and refractions (Pn) generated at the crust-mantle boundary, we first performed a
144 frequency-time analysis on selected good-quality traces by using the Gabor transform-like multi-filter
145 analysis technique [Dziewonski et al., 1969]. We used the Gabor transform algorithm available in the open
146 source software package Seismic Unix developed for the processing of active and passive seismic data by the
147 Center for Wave Phenomena at the Colorado School of Mines [Cohen and Stockwell, 2008]. This algorithm
148 provides a multi-filter representation of the instantaneous amplitude of seismic data in the time-frequency
149 domain. An input waveform is passed through an ensemble of Gaussian filters to produce a collection of
150 seismic traces, each representing a discrete frequency range in the input data. For each of these narrow
151 bandwidth traces, the instantaneous amplitude is related to the real part of the analytic trace, that is just the
152 original narrow bandwidth trace, and to its imaginary part, also called the *quadrature* trace, that is computed
153 by taking the Hilbert transform of the real part. Therefore, after computing the instantaneous amplitude of all
154 narrow bandwidth traces, the output is represented as a function of time and frequency.

155 We performed the Gabor transform-like multi-filter analysis on selected seismograms extracted from
156 the vertical component record sections arranged in Common Receiver Gather (CRGs). For each seismic
157 station and for different offset ranges, we selected seismic traces that satisfy two criteria: (i) best signal-to-
158 noise ratio, (ii) the arrival of the target phase (i.e., primary refracted waves or wide-angle reflections) is well
159 separated from secondary phases. The analysis was performed on 10 selected traces at least for each CRGs.
160 Based on the frequency content of the target seismic phases estimated by multi-filter analysis, we designed
161 optimal band-pass filters depending on the offset range and target phase.

162 We applied an automatic gain (RMS-type function) to outline very weak first arrivals that precede
163 large-amplitude post-critical reflections. Traces were tapered and then plotted with reduced times using
164 different velocities to discriminate crustal and mantle arrivals. All the processing was performed by using the
165 Seismic Unix free software package.

166 Then, vertical component CRGs were classified according to the signal-to-noise ratio, amplitude,
167 lateral coherence and continuity of the main phases (e.g. first arrivals travelling in sedimentary layers and
168 through the mid- and lower-crust, wide-angle crustal reflections, PmP reflections, Pn refractions).

169

170 3.2 Profile P02

171 All record sections, but CRG8, show usable seismic phases, which are more or less clear depending on
172 the distance from the coastline and local site conditions.

173 CRG3, located at 22014 m from the closest source, can be considered representative of the onshore
174 seismic data recorded in Apulia (Figure 5). In the following we describe the main phases identified on the
175 record section at increasing source-receiver distances.

176 First arrivals with apparent velocity comprised between 5.5 and 7.0 km/s are evident up to 50 km
177 offset (Figure 6). These arrivals can be interpreted as refracted waves travelling inside the Meso-Cenozoic
178 carbonate multilayer of the Apulia Platform, which has V_p around 5.5-6.0 km/s in the limestone sequences
179 and V_p around 6.5-6.7 km/s in the basal Triassic evaporites (see the Puglia 1 well sonic log reported by
180 Improta et al., [2000]). Frequency content of these shallow refractions ranges from 2 to 10 Hz.

181 Beyond 50 km offset, data show an evident decrease of the signal-to-noise ratio (Figure 6). Amplitude
182 and lateral coherence of first arrivals and early reflections are low, while apparent velocities of these arrivals
183 decrease rapidly toward the east (apparent velocity for first arrivals decreases down to 4.5-5.0 km/s). This
184 change in data quality correlates to the abrupt deepening of the sea floor that marks the transition between
185 the Apulia Platform and the Adriatic basin (between shot number 1300 and 1200; Figure 4). In addition, the
186 very low amplitude and apparent velocities of first arrivals may be related to lateral and/or vertical velocity
187 heterogeneities within the Apulian sedimentary cover. Indeed, we expect a lateral V_p change between
188 Mesozoic platform carbonates and coeval pelagic limestones in correspondence to the Apulia steep margin.
189 Furthermore, it is well known that the Apulia Platform overlies a low velocity layer consisting of Permo-
190 Triassic clastic sediments drilled at the base of the Triassic evaporites (V_p around 5.0-5.5 km/s; see Puglia 1
191 well in Improta et al. [2000]). Such a low- V_p layer should cause a shadow zone in the first-arrival branch, a
192 feature that reconciles with the abrupt decrease in amplitude and apparent velocity for shallow refractions
193 observed between 50 and 60 km offset (Figure 6).

194 Weak first arrivals with an apparent velocity larger than 7.0 km/s are visible between 65 and 70 km
195 offset with corrected traveltimes around 4.5 s (for reduction velocity of 8 km/s, Figure 5) or 3.5 s (for a
196 reduction velocity of 7 km/s, Figure 6). These arrivals may represent refractions from the top of the
197 crystalline basement, thereby below the low- V_p layer drilled under the base of the Apulia Platform [Improta
198 et al., 2000].

199 The offset range 70-80 km corresponds to a shadow zone (Figure 7). Even if data quality is quite good,
200 first arrivals are barely visible and coherent arrivals (with apparent velocities of 6.5-7.0 km/s) appear for
201 reduced times larger than 5.5-6.0 s (crustal refracted and wide-angle reflection waves). This shadow zone
202 may be indicative of a low V_p layer or of a low velocity gradient zone in the mid crust. These crustal phases
203 are visible up to 110 km and converge towards large amplitude PmP reflections. The mantle wide-angle
204 reflections exhibit excellent lateral coherence and continuity from 70 km to 120 km and have traveltimes
205 increasing with offset from 7.5 to 8.5 s (reduced times using a reduction velocity of 8 km/s; see Figure 7).

206 From 80 to 110 km offset, the first P-pulses could correspond to very weak and discontinuous arrivals
207 outlined by blue arrows in Figure 7. This interpretation is based on data recorded by station P2_R2 located at
208 15503 m from the closest shot (Figure 8). Section CRG2 shows a weak but lateral continuous refracted phase
209 between 80-102 km with apparent velocities of 6.8-7.0 km/s and reduced traveltimes of 4.2-4.5 s (see Figure
210 9). These crustal refractions again precede deeper crustal refracted phases that in turn tend asymptotically to
211 large amplitude PmP reflections with excellent lateral coherence and continuity from 70 km to 120 km offset
212 (Figures 9 and 10). Frequency content of the weak crustal refracted wave ranges from 4-5 to 8-9 Hz, while
213 PmP reflections range from 2-3 to 12-14 Hz, with a dominant frequency of 7-8 Hz (Figure 10).

214 Clear, large-amplitude PmP reflections characterize also the other common receiver gathers with the
215 exception of gather CRG8. Mantle wide-angle reflections can be easily picked at source-receiver distances
216 comprised between 70-80 and 100-120 km. Unfortunately, land stations along profile P02 lack mantle
217 refractions.

218 For what concerns first arrivals, upper crustal refractions travelling within the Apulia Platform can be
219 picked up to 40-50 km offset on CRG1 to CRG5. These first arrival traveltimes carry information on the
220 upper crustal velocity structure under the eastern margin of the Apulia Platform.

221

222 3.3 Profile P03

223 All record sections show crustal phases, mantle wide-angle refractions and mantle refractions. Data
224 recorded by station P03_R3 located at 24.6 km distance from the closest airgun shot shows the best signal-
225 to-noise ratio in the intermediate-large offset range (Figure 11). In the following, we describe the main
226 phases identified on the record section CRG3 at increasing source-receiver distances.

227 First arrivals with apparent velocities of 6.0-6.5 km/s can be picked from 24.6 km to about 50 km
228 offset (Figures 12). These refractions were travelling within the high-Vp Apulian carbonates and evaporites
229 (see the Gargano 1 well sonic log published by Improta *et al.* [2000]) progressively deteriorate with offset
230 and precede clear arrivals with apparent velocities around 6.7 km/s that could be related to refractions and
231 wide-angle reflections from the crystalline basement (Figure 12). First arrivals are hardly identifiable from
232 50 km to 60 km, and the basement refractions likely become first arrivals beyond 60 km. The resulting gap in
233 first arrivals around 55-60 km defines a clear shadow-zone (Figure 12) that suggests the presence of a low-
234 Vp layer. Such a layer might correspond to low-Vp sediments sandwiched between the Apulia Platform
235 carbonate multilayer and the underlying Paleozoic crystalline basement. This interpretation is consistent
236 with: (i) the regional-scale low-Vp layer resolved between the upper and mid crust by teleseismic receiver
237 functions computed for all stations of the National Seismic Network (in Italian: Rete Sismica Nazionale –
238 RSN [Michellini *et al.*, 2016]) installed in the Gargano Promontory and Apulia foreland [Amato *et al.*, 2014];
239 (ii) logs of the Gargano 1 well that drilled low-Vp Permo-Triassic clastic deposits underneath the Apulian
240 Triassic evaporites.

241 Amplitudes and apparent velocities of basement refractions rapidly decrease at offsets beyond 65-70
242 km (Figure 13). This observation relates strictly to the abrupt deepening of the sea floor to the east of shot
243 points 300-320 (Figure 4). Thus, the 70-85 km offset range is characterized by extremely weak first arrivals,
244 which can be identified after a careful processing, followed by large amplitude crustal refractions/reflections
245 and PmP arrivals (Figure 14). The apparent velocity of these subtle first arrivals, as well as of the deeper
246 crustal phases, is around 6 km/s, but this value is clearly underestimated due to the bathymetry that steeply
247 dips eastward.

248 Deep crustal refractions become, in turn, first arrivals beyond 95 km (Figure 15). These deep crustal
249 refractions tend asymptotically to PmP arrivals and are characterized by apparent velocities around 7.0 km/s
250 (beyond 95-100 km offset where the sea floor is regular). Frequency content of these weak crustal refractions
251 observed at large offset ranges from 4 to 10 Hz.

252 At offsets larger than 110 km, first arrivals correspond to mantle refractions that precede large
253 amplitude mantle reflections (Figure 11 and Figure 16). The frequency content is comprised between 3-4 and
254 8-9 Hz for Pn arrivals and between 3-4 and 11-14 Hz for PmP arrivals (Figure 10b). The Pn branch is
255 outlined by a clear knee point in the first arrival traveltimes curve (at around 108 km offset) and by typical
256 apparent velocities of 7.9-8.2 km/s for mantle refractions (Figure 16). The Pn phases have a fair signal-to-
257 noise ratio and lateral coherence between 108-115 km, 123-142 km, 161-177 km. Large amplitude PmP
258 arrivals are evident from 70 km to 140 km offset and have traveltimes increasing with offset from 6.7 to 8.2 s
259 (reduced times using a reduction velocity of 8 km/s; see Figure 11).

260 First arrivals associated to refracted waves travelling within the Apulia sedimentary layers, having
261 apparent velocities of 5.5-6.5 km/s, can be picked up to 40-45 km offsets on all CRGs.

262 Fair mantle refractions can be identified on processed common receiver gathers from CRG1 to CRG4
263 beyond about 100 km offset. Post-critical large-amplitude PmP arrivals, with good lateral continuity and
264 coherence characterize all five common receiver gathers. The PmP branch can be accurately picked at
265 source-receiver distances comprised between 60-80 and 120-150 km.

266

267 4. Discussions and Conclusions

268

269 The primary goal of ALPHA survey was the high-resolution tomographic imaging of the crust and
270 lithospheric mantle underneath the southern Adriatic Sea along three dense wide-aperture offshore profiles.

271 To illuminate the crust and crust-mantle boundary underneath the eastern side of the Apulia Platform, we
272 extended the two SW-NE profiles onshore by deploying temporary short-period stations in the Gargano
273 Promontory (profile P03) and Apulia region (profile P02).

274 We improved the signal-to-noise ratio by applying to the common receiver gather sections a
275 processing flow specifically designed to highlight crustal phases, mantle wide-angle reflections and mantle
276 refractions.

277 Our analysis of the processed CRG sections illustrates the high quality of the collected data.

278 The identification of first arrivals is complicated by shadow zones. An evident break in the first-arrival
279 curve observed on record sections of profile P03 at about 50-60 km offset (Figure 12) points to the presence
280 of a low-Vp layer in the upper crust above the crystalline basement. This finding is in agreement with the
281 low-Vp sediments drilled by two deep wells [Improta et al., 2000] and imaged by teleseismic receiver
282 functions as a low-Vs layer sandwiched between the Apulia Triassic evaporites and the crystalline basement
283 in the depth range 4-6 to 8-10 km [Amato et al., 2014].

284 The five stations of the Gargano transect recorded both clear PmP reflections and Pn arrivals. In
285 addition to the relevant mantle phases that were even recorded from the opposite end of the shot line
286 (Figure 11), crustal refraction and reflected arrivals can be identified and accurately picked on all record
287 sections in the small to intermediate offset range. Thus, the land deployment allows to extend the volume
288 sampled by seismic rays 33 km to west of the closest airgun shot. The recorded onshore data carry
289 information on the upper crustal velocity structure in the Gargano Promontory, while the joint modelling of
290 Pn and PmP phases allows to illuminate a portion of the crust-mantle boundary that extends 35-40 km
291 eastward from the coastline. Preliminary modelling of mantle wide-angle reflections and mantle refractions
292 recorded by OBH/OBS and INGV land stations indicates that the crust-mantle boundary is about 34 km deep
293 under the Gargano coastline and gently dips eastward [Figure 17, Dannowski et al., 2016]. This depth value
294 is in good agreement with the depth of 30-32 km estimated by Amato et al. [2014] by using teleseismic
295 receiver functions recorded at two INGV permanent stations located in the Gargano Promontory.

296 Along the Apulia transect, seven out of eight stations recorded clear crustal phases and mantle wide-
297 angle reflections characterized by excellent lateral continuity and coherence. The farthest station with usable
298 data P02_R7 is located at 47 km distance from the western ending of the marine seismic profile and recorded
299 PmP arrivals between 70 and 100 km offset (corresponding to a shooting distance of 23-53 km from the
300 beginning of the offshore profile). Therefore, PmP arrivals recorded by station P02_R7 illuminate an about
301 30 km long portion of the crust-mantle boundary located onshore underneath the Apulia Platform. Taken
302 together, PmP traveltimes picked from the closest station (P02_R1) to the farthest one (P02_R7) provide
303 constraints on the crust-mantle boundary underneath the western side of the Adriatic basin and the Apulia
304 Platform.

305 Differently from profile P03, no land station recorded mantle refractions along the P02 profile. We
306 speculate that the lack of Pn arrivals might be an effect of a deeper crust-mantle boundary that would shift
307 the knee point between crustal and mantle refractions towards very large offset traces characterized by a
308 lower signal-to-noise ratio. This hypothesis reconciles with PmP traveltimes that are larger for P02 stations:
309 PmP arrival times at about 70 km offset are equal to 6.7 s for station P03_R3 and to 7.5 s for station P02_R3
310 (see Figures 6 and 12).

311 The observation of Pn arrivals at far offset (up to 170 km, Figure 16) and of very clear mantle
312 reflections in a large offset range on land record sections (Figures 6 and 12) are not obvious or expected
313 results. We remark that such results are valuable in the light of the energy of the used airgun source (i.e., 84
314 litres) that is ordinary for academic surveys and of the large distance of land stations from the coastline (47
315 km and 33 km for profile P02 and P03, respectively). Comparable example of good quality mantle phases
316 recorded by land stations during wide-angle marine seismic surveys in Italian seas are rare [Prada et al.,
317 2015; Dellong et al., 2018]. We believe that the acquisition of good quality data even at very large offset has
318 been possible thanks to excellent local conditions of the recording sites chosen after a careful selection, as
319 well as to low seismic attenuation of the Apulia continental crust.

320

321 **Acknowledgments**

322 Comments by reviewers Adrià Meléndez and Flavio Accaino helped to improve the manuscript and are
323 thankfully acknowledged. We thank the Editor Federica Riguzzi for useful suggestions.
324

325

326 **References**

327

328 Amato, A., I. Bianchi and N. Piana Agostinetti (2014). Apulian crust: Top to bottom. *Journal of*
329 *Geodynamics*. 82. 10.1016/j.jog.2014.09.007.

330 Bennett, R. A., S. Hreinsdóttir, G. Buble, T. Bašić, Ž. Bačić, M. Marjanović, G. Casale, A. Gendaszek
331 and D. Cowan (2008). Eocene to present subduction of southern Adria mantle lithosphere beneath the
332 Dinarides. *Geology*, 36(1), 3-6. DOI: 10.1130/G24136A.1

333 Cohen, J. K. and J. W. Stockwell (2008). CWP/SU: Seismic Un*x Release No. 4.0: an open source
334 software package for seismic research and processing. Center for Wave Phenomena, Colorado School of
335 Mines.

336 Dannowski, A., H. Kopp, B. Schurr, L. Improta, C. Papenberg, A. Krabbenhöft and A. Argnani
337 (2016). Amphibious seismic study on the crustal structure of the Adria. 41st CSIEM Congress, Kiel
338 Germany, September 2016.

339 Dellong, D., F. Klingelhoefer, H. Kopp, D. Graindorge, L. Margheriti, M. Moretti, et al. (2018).
340 Crustal structure of the Ionian basin and eastern Sicily margin: Results from a wide-angle seismic survey.
341 *Journal of Geophys. Res. Solid Earth*, 123, 2090–2114. <https://doi.org/10.1002/2017JB015312>.

342 D'Agostino, N., A. Avallone, D. Cheloni, E. D'Anastasio, S. Mantenuto and G.
343 Selvaggi (2008). Active tectonics of the Adriatic region from GPS and earthquake slip vectors. *J. Geophys.*
344 *Res.*, 113, B12413, doi:10.1029/2008JB005860.

345 Dziewonski, A., S. Bloch and G. Landisman (1969). A technique for the analysis of transient seismic
346 signals. *Bull. Seism. Soc. Am.*, 59, 1, 427-444.

347 Improta, L., G. Iannaccone, P. Capuano, A. Zollo and P. Scandone (2000). Inferences on the upper
348 crustal structure of Southern Apennines (Italy) from seismic refraction investigations and subsurface data.
349 *Tectonophys.*, 317, p. 273–297.

350 Kopp, H., A. Dannowski, A. Argnani, I. Dasović, I. Dumke, J. Elger, E. Flueh, B. Frey, M.R. Handy,
351 J. Karstens, M. Kordowski, A. Krabbenhoeft, J. Mögeltönder, C. Papenberg, L. Planert, K.P. Steffen, J.
352 Stipčević, K. Ustaszewski, W. Weinrebe, T. Wiskandt and T. Zander (2013). ADRIA LITHOSPHERE
353 INVESTIGATION ALPHA - Cruise No. M86/3 - January 20 - February 04, 2012 - Brindisi (Italy) -
354 Dubrovnik (Croatia) (Version 1.0). DFG-Senatskommission für Ozeanographie.
355 https://doi.org/10.2312/cr_m86_3.

356 Michelini, A., L. Margheriti, M. Cattaneo, G. Cecere, G. D'Anna, A. Delladio, M. Moretti, S. Pintore,
357 A. Amato, A. Basili, A. Bono, P. Casale, P. Danecek, M. Demartin, L. Faenza, V. Lauciani, A.G. Mandiello,
358 A. Marchetti, C. Marcocci, S. Mazza, F.M. Mele, A. Nardi, C. Nostro, M. Pignone, M. Quintiliani, S. Rao,
359 L. Scognamiglio and G. Selvaggi (2016). The Italian National Seismic Network and the earthquake and
360 tsunami monitoring and surveillance systems. *Adv. Geosci.*, 43, 31-38, doi:10.5194/adgeo-43-31-2016.

361 Prada, M., V. Sallares, C.R. Ranero, M.G. Vendrell, I. Grevemeyer, N. Zitellini and R. De Franco
362 (2015). The complex 3-D transition from continental crust to backarc magmatism and exhumed mantle in the
363 Central Tyrrhenian basin. *Geophys J. Int.*, 203, Issue 1, 63–78, <https://doi.org/10.1093/gji/ggv271>

364

365 **TABLES**

366

367 **Table 1.** Coordinates of P02 profile land stations (see map in Figure 1 and Figure 2).

Station code	Latitude (°N)	Longitude (°E)	Altitude (m)
R1	17° 44.6948'	40° 42. 5696'	64
R2	17° 39.9490'	40° 40.0390'	141
R2	17° 39.5720'	40° 35.9850'	129
R4	17° 35.6138'	40° 34.5611'	210
R5	17° 33.2460'	40° 30.5966'	161
R6	17° 31.9630'	40° 27.6220'	141
R7	17° 30.4440'	40° 24.3183'	148
R8	17° 25.9484'	40° 21.0378'	20

368

369

370 **Table 2.** Coordinates of P03 profile land stations (see map in Figure 1 and Figure 3).

Station code	Latitude (°N)	Longitude (°E)	Altitude (m)
R1	16° 08.9233'	41° 51.3008'	104
R2	16° 05.0356'	41° 51.1542'	355
R2	15° 59.7018'	41° 49. 9453'	733
R4	15° 58.2476'	41° 50.0883'	754
R5	15° 53.5240'	41° 50.1910'	330

371

372

373

374

375

376

377

378

379

380

381

382

383

384

385

386

387

388

389 **CATPIONS**

390

391 **Figure 1.** The map shows the three seismic refraction profiles collected during the FS METEOR cruise
392 M86/3 in the central-southern Adriatic Sea. Blue triangles are land stations that recorded the airgun shots.
393 Black triangles are OBH/OBS instruments (modified from Kopp et al. [2013]).

394

395 **Figure 2.** Location of INGV stations along the Apulia transect (profile P02). The white and yellow lines
396 indicate the offshore profile P02 and its land prolongation, respectively. Blue symbols and labels (P2_R1 to
397 P2_R8) denote INGV land stations, numbers (01, 02, etc) denote position of OBH/OBS (modified from
398 Google Earth, 2017).

399

400 **Figure 3.** Location of INGV stations in the Gargano Promontory (profile P03). The white and yellow lines
401 indicate the offshore profile P03 and its land prolongation, respectively. Blue symbols and labels (P3_R1 to
402 P3_R5) denote INGV stations, numbers (01, 02, etc) denote OBH/OBS (modified from Google Earth, 2017).

403

404 **Figure 4.** Sea floor depth along P02 (top) and P03 (bottom) as a function of the shot number and shot
405 position along the profile.

406

407 **Figure 5.** P02-CRG3: traces are band-pass filtered ($f=3-5-9-12$ Hz) and plotted with reduced times ($V_r=8$
408 km/s). Yellow arrows denote first arrivals (refractions from the Apulian sedimentary sequence and the top of
409 the crystalline basement), blue arrows possible weak first-arrivals (refracted waves through the mid crust),
410 red arrows large amplitude PmP arrivals. The red dashed lines outline the offset range of the data plotted in
411 Figure 6, while the red continuous rectangle delimits data showed in Figure 7.

412

413 **Figure 6.** P02-CRG3: zoom on the small-to-intermediate offset range showing refracted waves
414 from the sedimentary layers. Traces are band-pass filtered ($f=3-5-9-12$ Hz) and plotted with reduced
415 times ($V_r=7$ km/s). Yellow arrows denote first arrivals.

416

417 **Figure 7.** P02-CRG3: traces in the 65-124 km offset range. Traces are band-pass filtered ($f=3-5-9-12$ Hz)
418 and plotted with reduced times ($V_r=8$ km/s). Yellow arrows denote first arrivals, blue arrows possible first-
419 arrivals (refracted waves through the mid-lower crust), red arrows clear PmP arrivals. The shadow zone is
420 outlined by the green circle.

421

422 **Figure 8.** P02-CRG2: traces are band-pass filtered ($f=2-3-8-10$ Hz) and plotted with reduced times ($V_r=8$
423 km/s). Yellow arrows denote first arrivals (refractions from the Apulian sedimentary sequence), blue arrows
424 weak first-arrivals of refracted waves through the mid crust, red arrows high-quality PmP reflections.

425

426 **Figure 9.** P02-CRG2: this zoom on the 73-103 km offset range allows outlining the weak and continuous
427 first-arrivals (grey arrows) that likely correspond to a refracted phase travelling in the mid-crust.

428

429 **Figure 10.** Frequency-time analysis (Gabor Transform) performed on selected seismograms. (a) P02-CRG2,
430 seismogram recorded at 91.1 km offset showing the first arrival of the refracted wave through the mid-crust
431 and the large amplitude, wide-angle PmP reflection; (b) P03-CRG3, seismogram recorded at 134.2 km offset
432 showing both mantle refraction (P_n) and reflection (PmP).

433

434 **Figure 11.** P03-CRG3: traces are band-pass filtered ($f = 4\text{-}5\text{-}9\text{-}11$ Hz) and plotted with reduced times ($V_r = 8$
435 km/s). This plot displays traces up to 170 km offset. Arrows outline first arrivals: refractions from Apulia
436 sedimentary layers (yellow), large-to-weak refractions possibly from the Apulia crystalline basement (blue),
437 refractions/reflections from the mid-lower crust (blue), mantle refractions (P_n , light blue), large amplitude
438 wide-angle mantle reflections (P_mP , red). The red dashed rectangle delimits data plotted in Figure 14, the red
439 dotted rectangle data in Figure 15, the red continuous rectangle data in Figure 16.

440

441 **Figure 12.** P03-CRG3: zoom on traces between 24633 m and 63000 m offset. Data are band-pass filtered
442 ($f=2\text{-}3\text{-}10\text{-}12$ Hz) and plotted with reduced times ($V_r=6.5$ km/s). Yellow arrows denote refracted waves from
443 the Apulia sedimentary layers (presumably from the high- V_p Triassic evaporites), blue arrows refractions
444 possibly from the Apulia crystalline basement. The “basement” refractions likely become first arrivals
445 beyond 60 km offsets. The yellow circle outlines a shadow zone.

446

447 **Figure 13.** P03-CRG3: traces from 45 to 90 km offset. Data are band-pass filtered ($f=4\text{-}5\text{-}9\text{-}11$ Hz) and
448 plotted with reduced times ($V_r=8$ km/s). The yellow circle highlights the region where the amplitude of
449 basement refractions (blue arrows) abruptly decreases. White and red arrows denote large-amplitude crustal
450 refracted/reflected waves and P_mP arrivals, respectively. The red rectangle bounds data showed in Figure 14.

451

452 **Figure 14.** P03-CRG3: zoom on traces characterized by very weak first arrivals (dashed line and arrows)
453 likely corresponding to a refracted wave from the crystalline basement. Data are band-pass filtered ($f=4\text{-}5\text{-}9\text{-}$
454 11 Hz) and plotted with reduced times ($V_r=8$ km/s).

455

456 **Figure 15.** P03-CRG3: zoom on the large offset data. Arrows denote extremely weak refracted wave from
457 the basement (blue), refractions from the mid-lower crust that become first arrivals beyond 95 km offset
458 (white), mantle wide-angle reflections (red), mantle refractions (light-blue) representing first arrivals beyond
459 110 km offset.

460

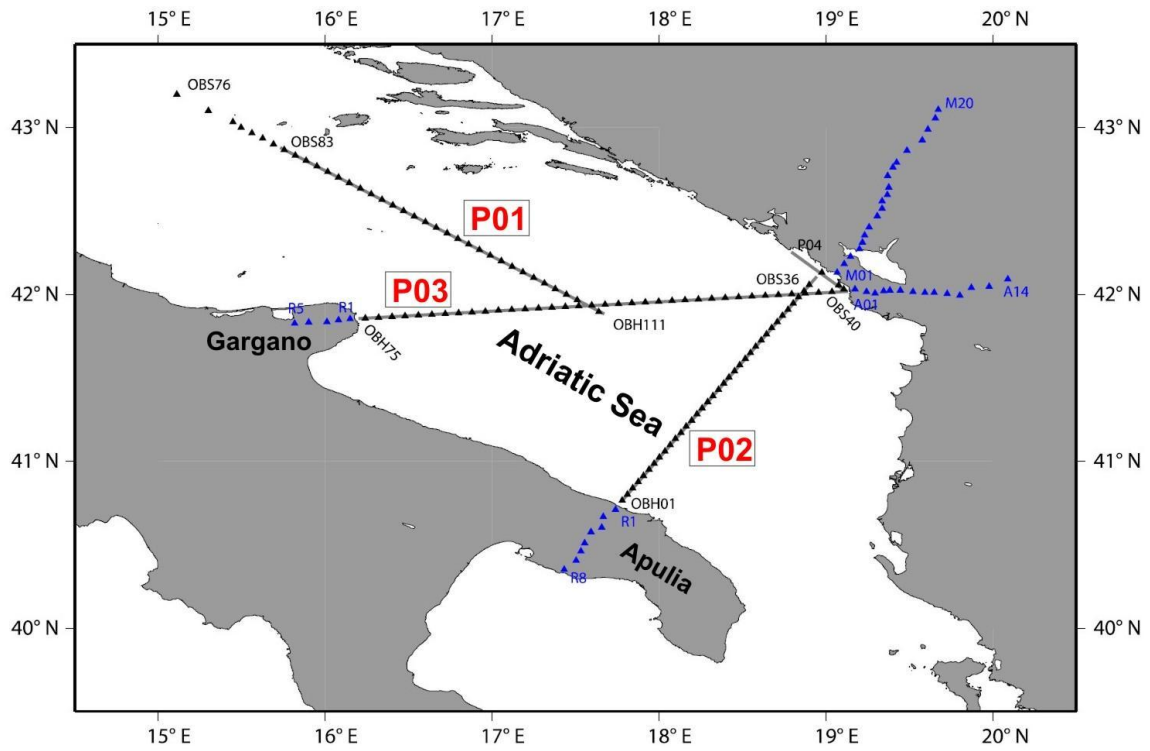
461 **Figure 16.** P03-CRG3: zoom on the far offset data showing P_n arrivals (light-blue arrows). The white arrows
462 indicate deep crustal refracted waves, red arrows mantle reflections. Data are band-pass filtered ($f=3\text{-}4\text{-}8\text{-}10$
463 Hz) and plotted with reduced times ($V_r=8$ km/s). A gain (RMS function, time-window of 1.0 s) is applied to
464 data to evidence weak P_n arrivals.

465

466 **Figure 17.** V_p model along the western portion of the P03 profile determined by preliminary modelling of
467 refraction and wide-angle reflection arrival times using marine and land stations [modified from Dannowski
468 et al., 2016]. Yellow triangles denote marine and land stations used for data modelling. Note that this
469 preliminary model does not include yet a low- V_p layer under the Apulia Platform.

470 **FIGURES**

471

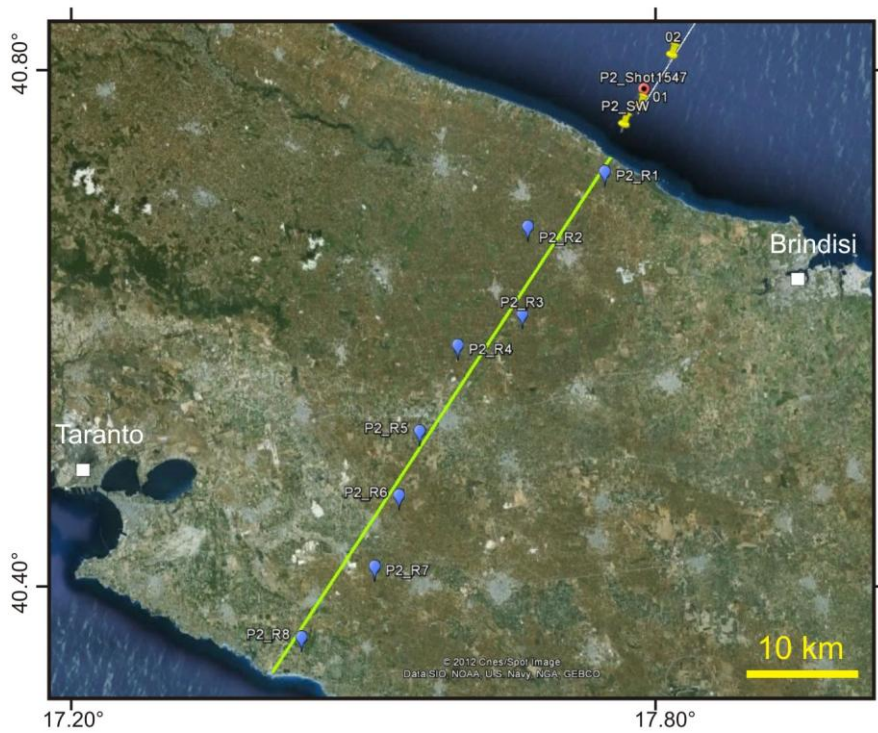


472

473

474

Figure 1



475

476

477

Figure 2

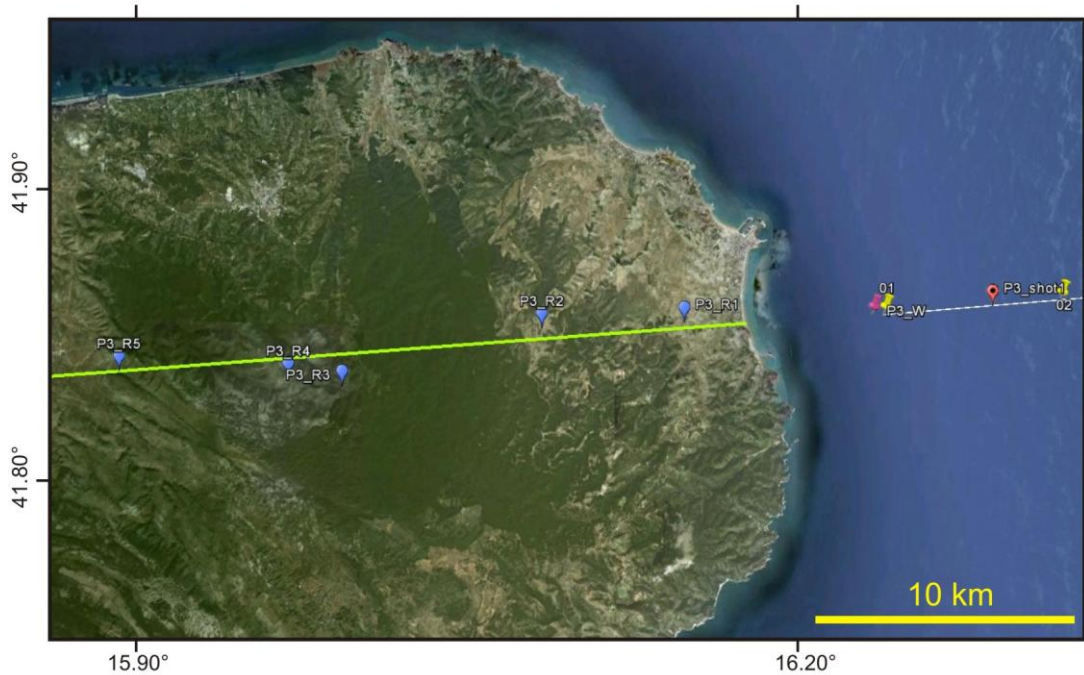


Figure 3

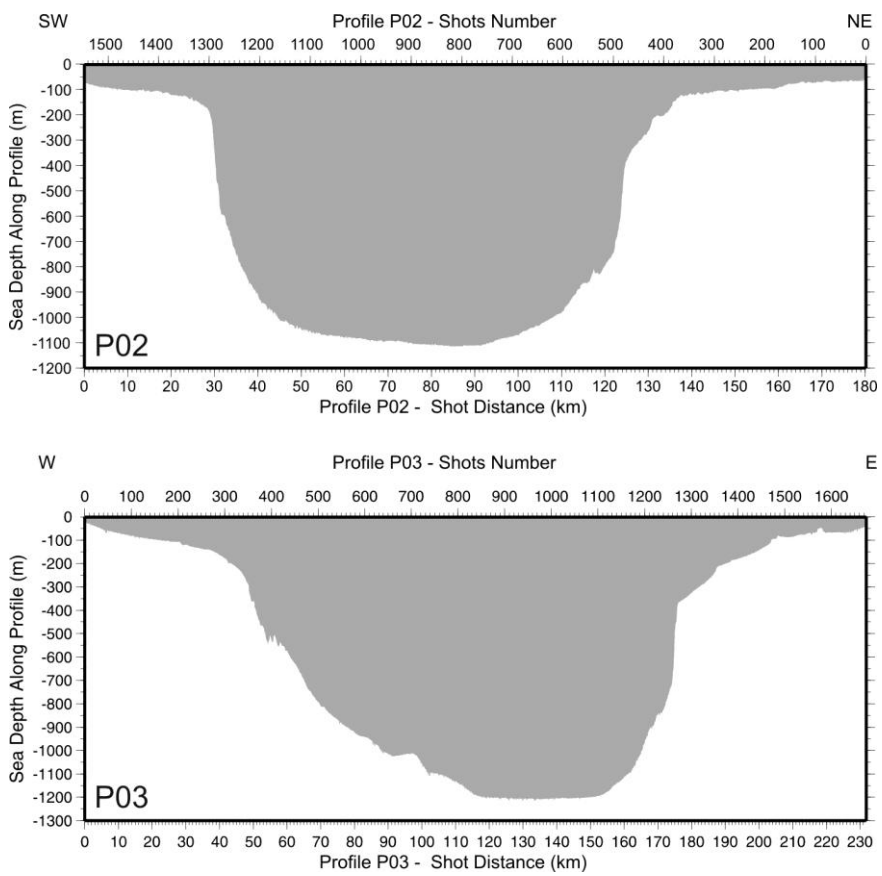


Figure 4

478
479
480

481
482
483
484

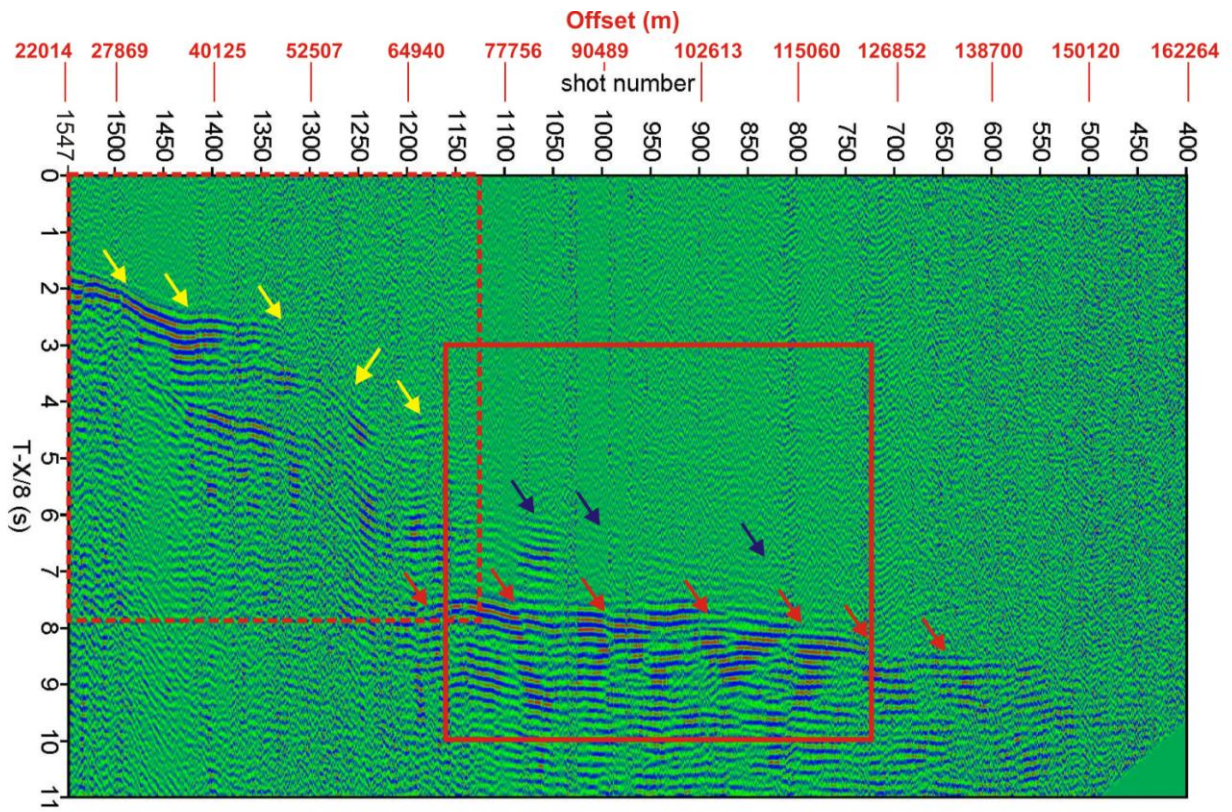


Figure 5

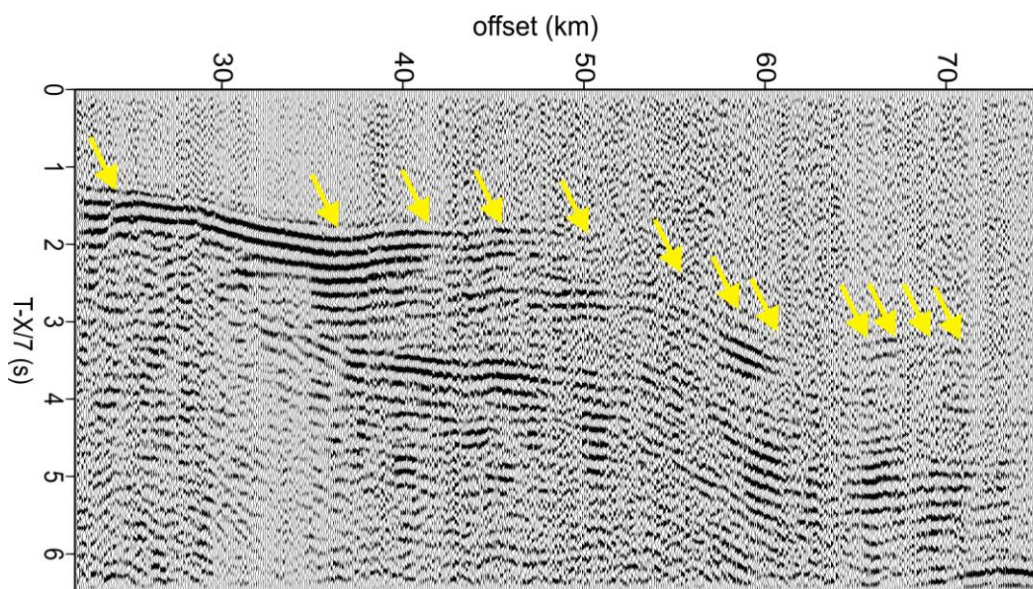
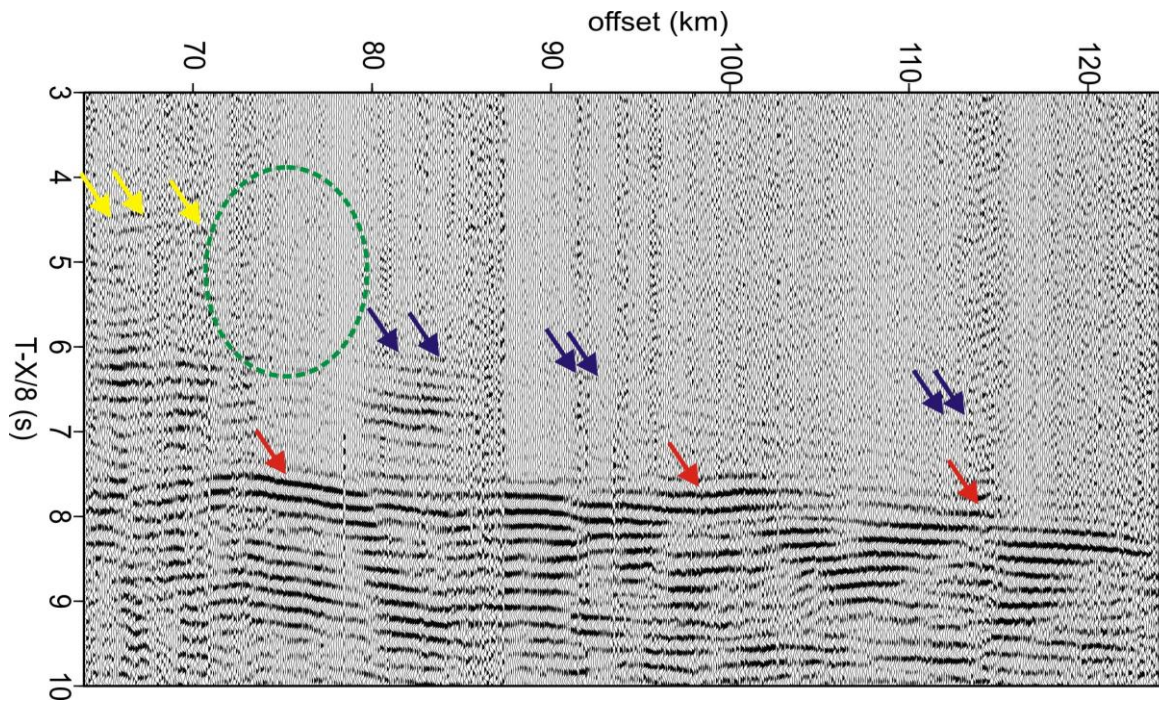
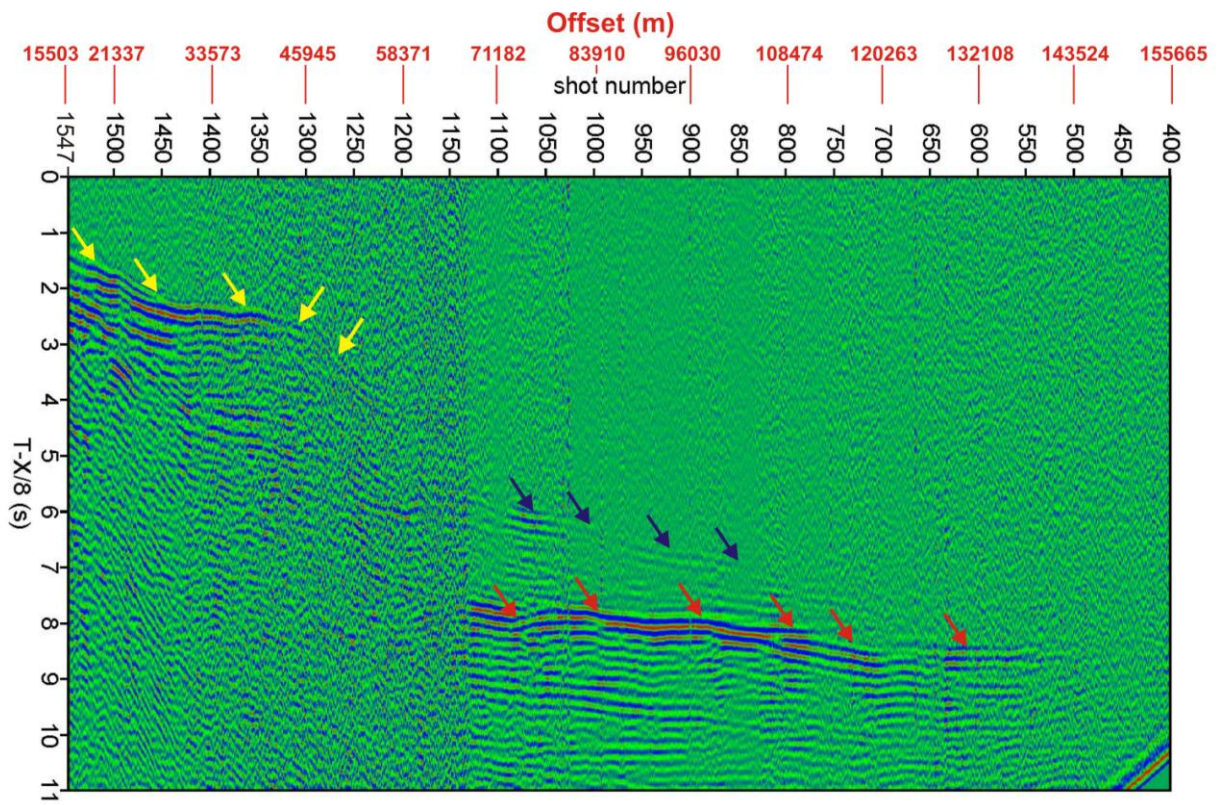


Figure 6



493
494
495

Figure 7



496
497

Figure 8

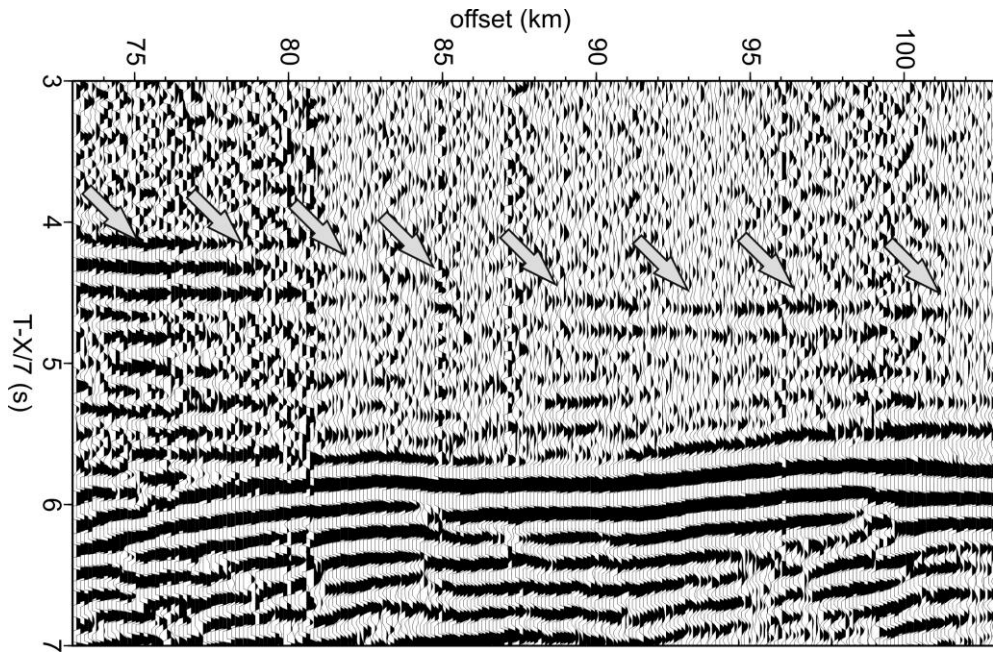


Figure 9

498
499
500

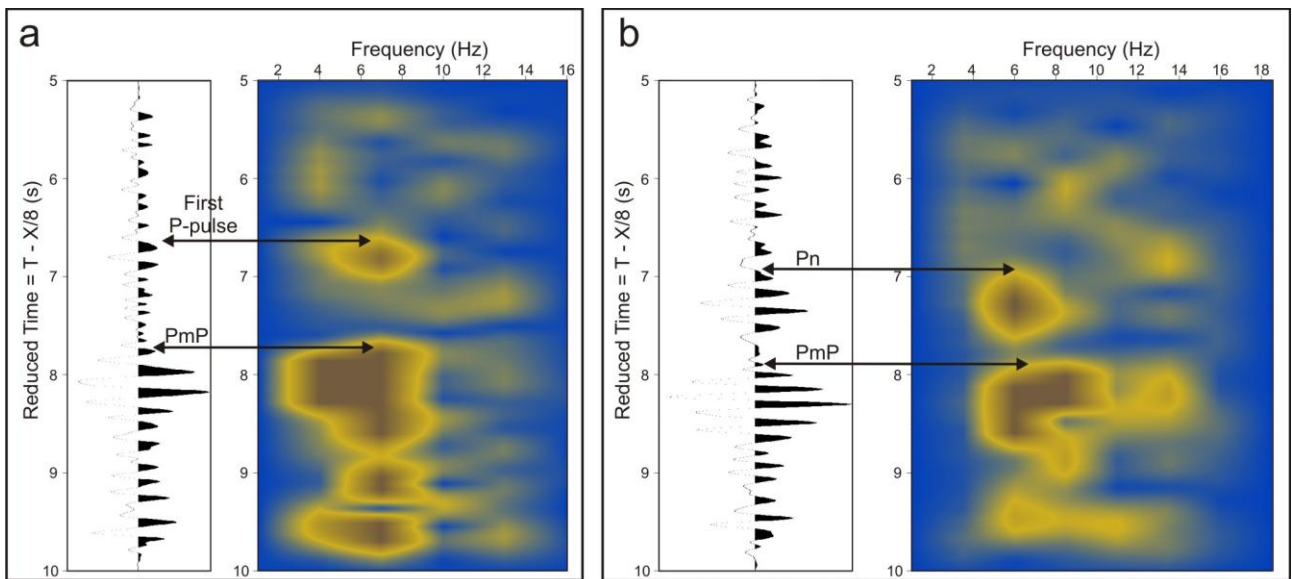
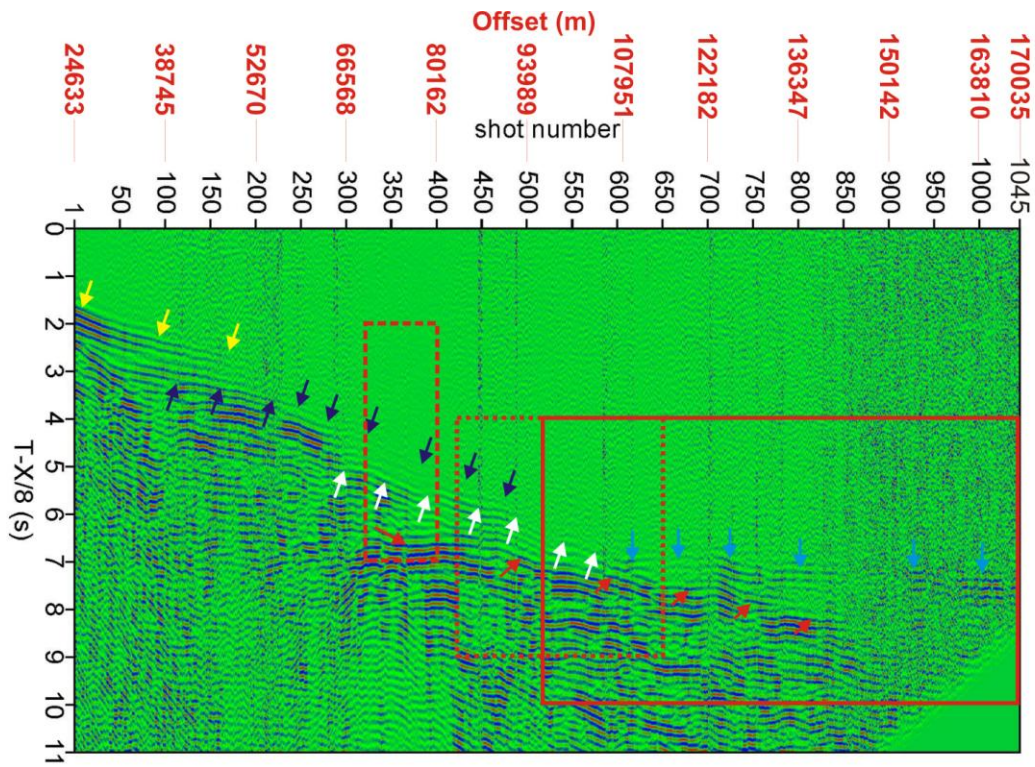


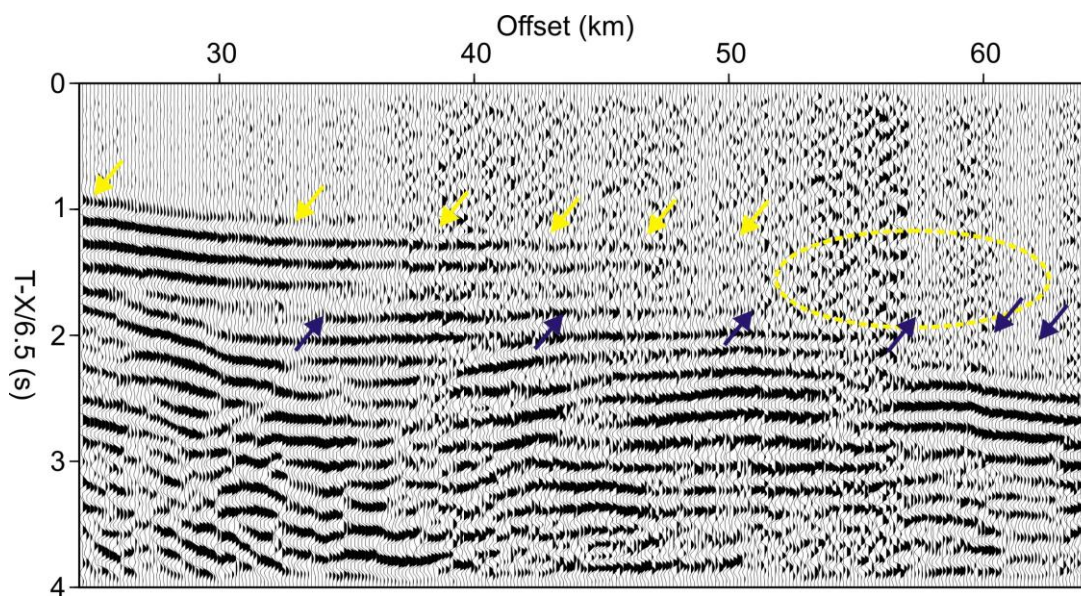
Figure 10

501
502
503



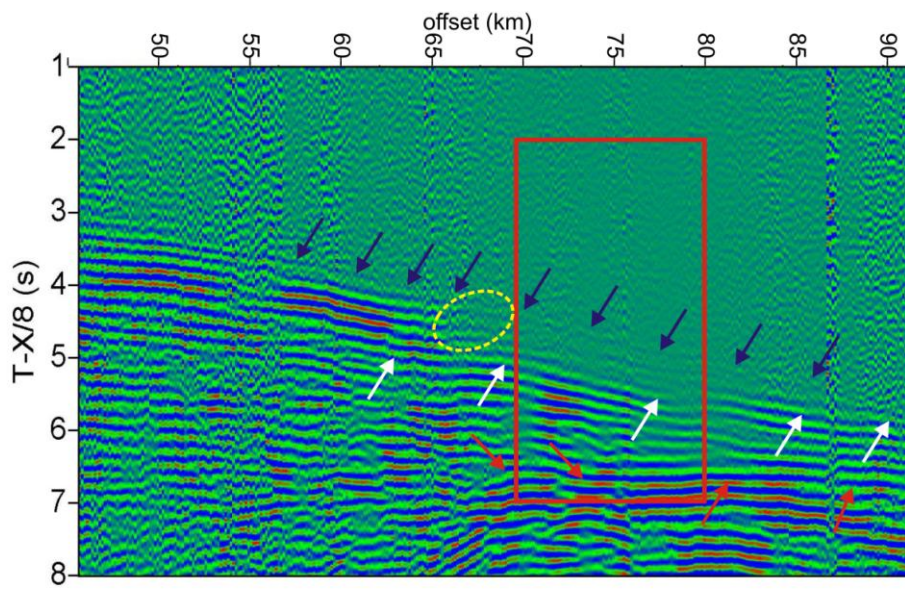
504
505
506
507

Figure 11



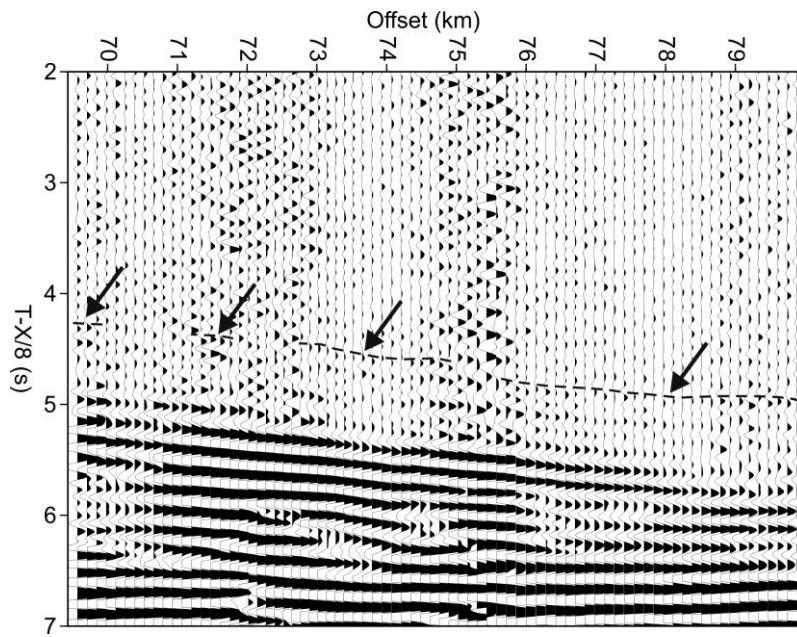
508
509
510
511

Figure 12



512
513
514

Figure 13



515
516

Figure 14

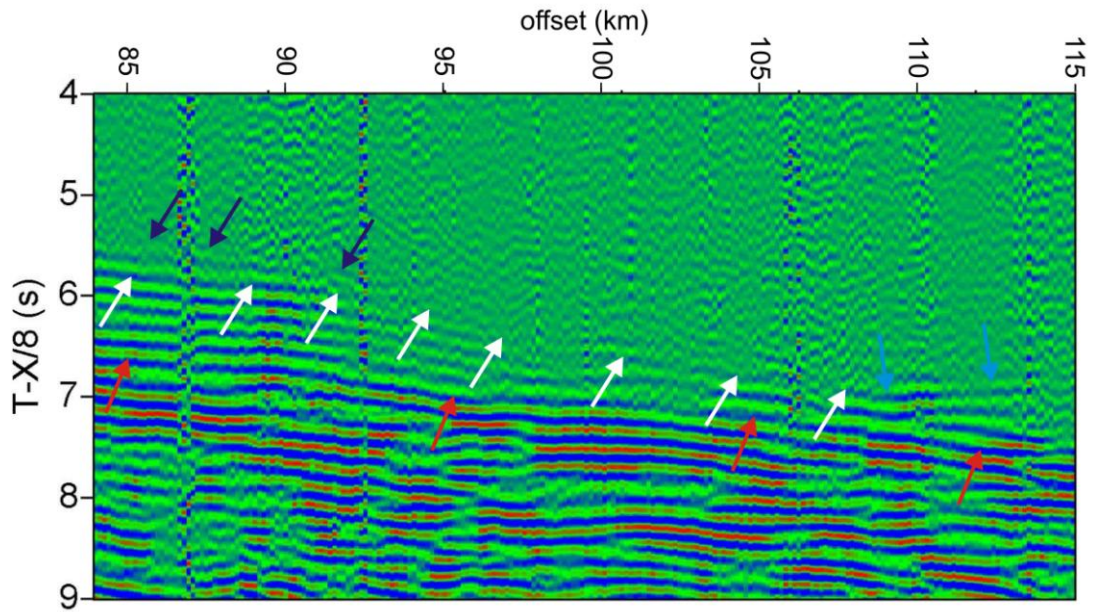


Figure 15

517
518
519
520

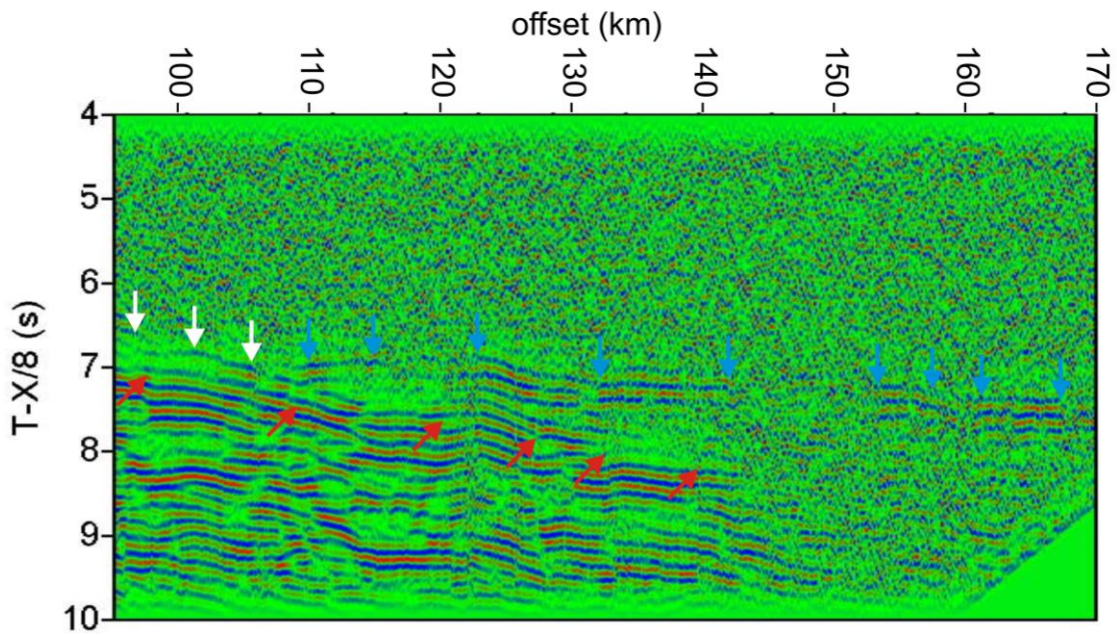
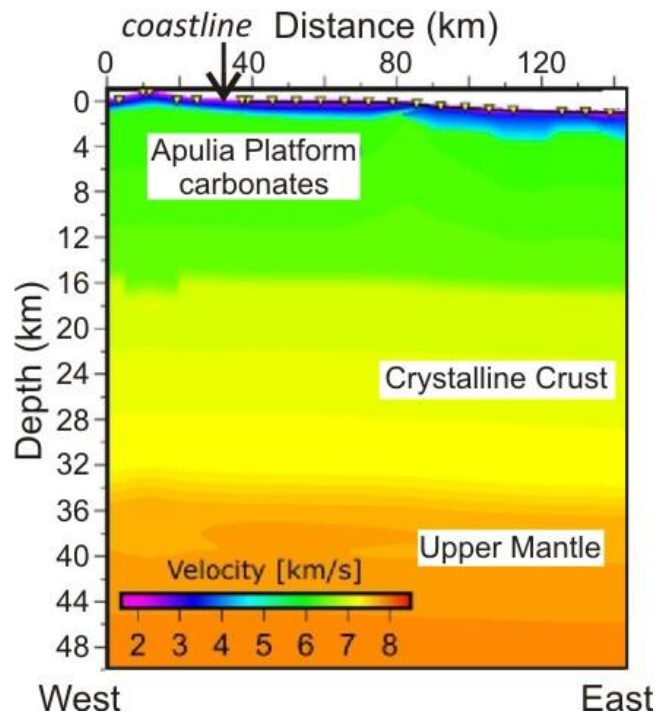


Figure 16

521
522
523

Gargano Promontory



524
525
526

Figure 17